

# Simulation of the $\beta$ setup of the SSD group

Jared Barron

August 25, 2017

## 1 Introduction

To reconstruct the events occurring in the LHC, experiments like ATLAS and CMS require high precision in tracking the resulting particles' trajectories. Both experiments make use of silicon sensors to reconstruct the paths of particles to within a few microns. The response of these sensors to ionizing particles must be well-understood in order to achieve this precision. Further development of silicon detector technologies is ongoing. One important characteristic of silicon detectors is the distribution of energy that minimum ionizing particles deposit in them as they pass through, especially as a function of the sensor's thickness. This measurement is conducted by exposing the sensors to a collimated beam of particles from a radioactive source and recording the output.

The objective of this study was to first implement a simulation in GEANT4 of the setup used by the SSD group to conduct such measurements. This simulation was then to be compared to theoretical results from the often-quoted paper by Bichsel [1] on energy deposition in silicon sensors of ionizing radiation, as well as measurements of the energy deposition distribution taken using the apparatus being simulated.

## 2 Setup

The apparatus consists of a radioactive source suspended above the silicon sensor being measured. The silicon sensor's signal is read out using a charge sensitive amplifier and an oscilloscope that records the signal waveforms. Data acquisition is dependent on a trigger system which comprises a scintillator coupled to a photomultiplier located after the sensor in the path of the particles from the radioactive source. The trigger is set as a voltage threshold on the signal from the photomultiplier. The geometry is held in place with supporting pieces anchored

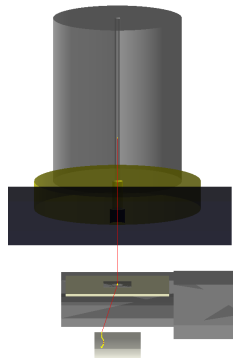


Figure 1: Geometry of the Susi setup and simulated event

to the interior of a climate chamber, which contains the entire apparatus, and supports multiple types of measurements, including capacitance vs voltage and current vs voltage across a wide range of temperatures. A more comprehensive description can be found in [2].

## 3 Simulation

The Source Simulation software from SiLab University Bonn [3], was downloaded and modified for simulation of the measurement apparatus - also known as Susi. The physical components of the apparatus which are near the path between radioactive source and sensor were measured and implemented in the simulation. These components included the housing of the source, the brass collimator, the plexiglass platform holding the collimator, the PCB upon which the sensor is mounted, the aluminum bracket holding said PCB, and the scintillator attached to the photo-multiplier used for triggering below the sensor. The records of exactly what material was used for the scintillator were not available, so it was simulated as polyethylene plastic. Figure 1 shows the simulated geometry, and a particle's trajectory through the detector.

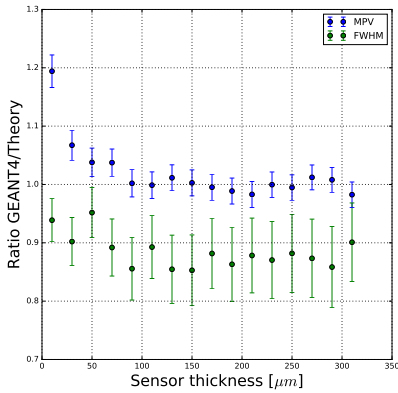


Figure 2: Ratio of simulated energy deposited in sensor by MIPs to expected value.

The simulation can generate specific particles with a given initial position and orientation, and draw energies from a distribution. It can also simulate the radioactive source and decay itself.

The first test performed, to assess the accuracy of GEANT4 in simulating the response of silicon to ionizing radiation, was to record the distribution of total energy deposited in silicon sensors of varying thickness by 3.2 GeV electrons. The most probable value and full-width at half-maximum from each distribution were recorded and compared with the values given in [1], which provides formulae as a function of thickness for particles above  $\beta\gamma = 500$ : equivalent to 250 MeV for electrons.

It was found that GEANT4 produces values consistent with Bichsel for the MPV at thicknesses  $> 100 \mu\text{m}$  but consistently underestimates the FWHM for MIPs, as shown in Figure 2. Errors for MPV were estimated at one bin width of the histogram used, and two bin widths for FWHM.

## 4 Trigger Calibration

Because data acquisition is triggered on the voltage output from the photomultiplier, for a meaningful comparison to be made between simulation and experiment, an equivalent condition must be applied to the events simulated. The most closely related variable accessible in the simulation is the energy deposited in the scintillator. The assumption was made that this deposited energy,  $E_{dep}$  is proportional to the signal

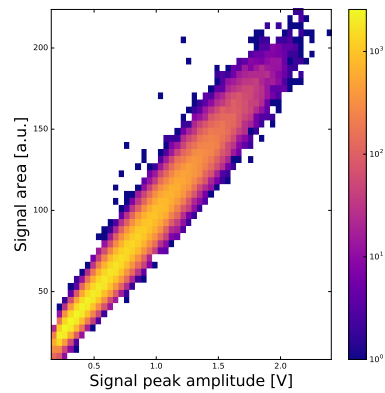


Figure 3: Comparison of signal amplitude vs area from photomultiplier.

from the photomultiplier coupled to the scintillator.

Operating the setup without the sensor in place, various radioactive sources were used to attempt to determine this proportionality. The goal was to compare the results to simulation, and use either peak amplitude or integrated charge from the photomultiplier as a proxy for  $E_{dep}$ . As can be seen from Figure 3, the two are linearly correlated, so peak amplitude was used as the observable for the tests performed in this work due to its more direct relation to the trigger level.

**Sodium 22** An Na-22 source was placed above the scintillator, and 8192 waveforms were recorded, with a trigger threshold of 200 mV. The observed energy spectrum of radiation from Na-22 is expected to have a peak at 511 keV from positron annihilation, 1.27 MeV due to gammas from a nuclear energy level transition in the Ne-22 product of the beta decay, and a continuous spectrum across energy from Compton scattering, with Compton shoulders at approximately 340 and 1068 keV. It was hoped that identification of these features in the pulse height distribution from the photomultiplier would allow a constant of proportionality to be found for converting energy deposited into peak output voltage.

As can be seen in Figure 4 the expected peaks are absent, but there are features similar to the expected Compton shoulders. When the same situation was simulated, the distribution of Figure 5 was obtained.

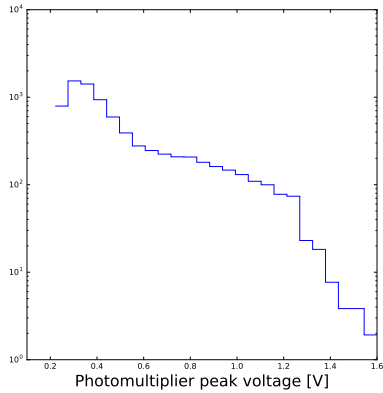


Figure 4: Observed sodium trigger pulse height distribution.

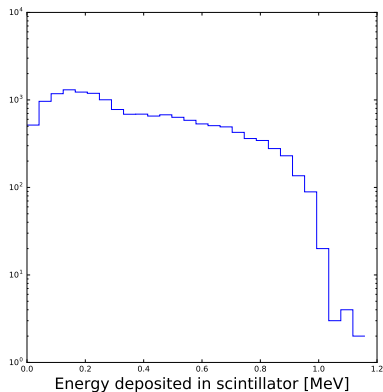


Figure 5: Simulated sodium trigger energy deposition distribution.

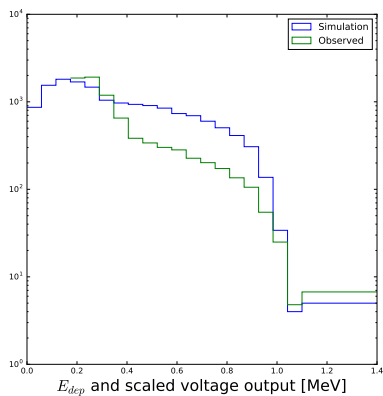


Figure 6: Simulated energy deposited and scaled observed voltage in scintillator.

The experimental and simulated data collected in the no-sensor geometry with a sodium-22 source were normalized to each other by setting the peak values equal to each other when binned in a histogram. A fit was then performed to minimize the Pearson's  $\chi^2$  goodness of fit test statistic between the two histograms, allowing a scaling multiplicative factor on the observed voltage values to vary. The best-fit value produced by the minimizer was 0.744 MeV/V. Figure 6 shows the result of fitting the histograms together. The Compton shoulder corresponding to 1.27 MeV gammas coincides particularly well between simulation and observation after the fit.

**Strontium 90** Measurements were also taken with a Sr-90 source, which undergoes beta decay first to Y-90 with a decay energy of 0.546 MeV, then to Zr-90 with a decay energy of 2.28 MeV. It was expected that the distribution of peak voltage would have a shoulder corresponding to the upper limit on energy deposited by electrons from the strontium decay, and a sharp drop-off corresponding to the termination of the spectrum of electron energies from yttrium decay. Approximately  $1.55 \times 10^5$  samples were collected with a trigger condition of 100 mV. Figure 7 shows the distribution of peak voltages obtained.

With the same geometry implemented in GEANT4, a simulation recording the energy deposited in the scintillator was performed. Figure 8 shows the distribution obtained. It matches the a priori expectation, but not the observed distribution.

The same comparison was made with the sensor in place. Figure 9 shows the simulated and observed spectra on the same plot. It is notable that the shape of the simulated distribution changes drastically, while experimentally the shape of the distribution of voltage output from the photomultiplier stays largely the same. Based on how the low-energy peak in the simulated distribution is suppressed by the presence of material between the source and the scintillator, the difference between observation and simulation in the no-sensor case can likely be attributed to small details in the source's housing that are not simulated, but have a large impact on the energy distribution of particles reaching the sensor and scintillator.

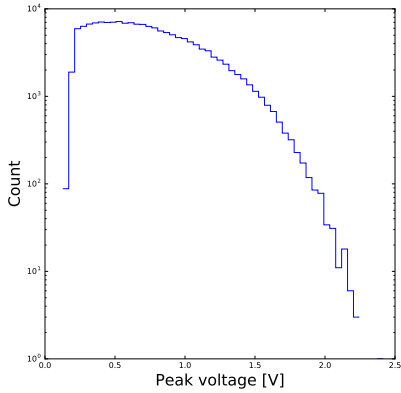


Figure 7: Observed strontium trigger pulse height distribution.

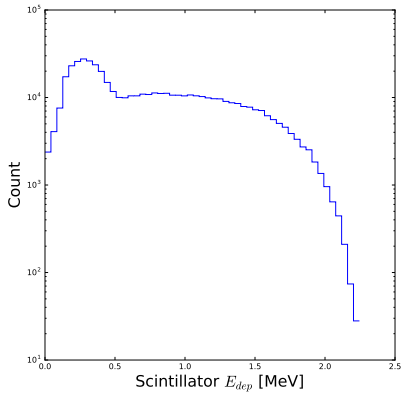


Figure 8: Simulated strontium trigger energy deposition distribution.

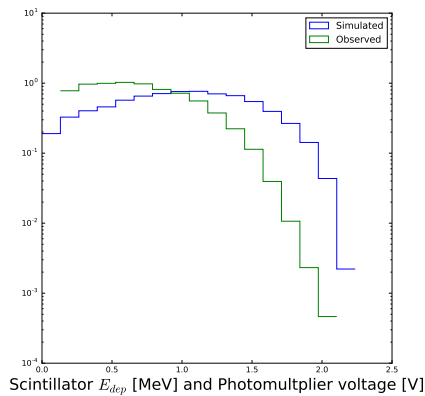


Figure 9: Observed and simulated trigger response with  $280\mu\text{m}$  sensor.

**Other Sources** Measurements were also taken with a Ru-106 source, but its activity was so low that insufficient statistics could be gathered to perform the same comparison as with the other sources.

## 5 Measurements with sensor

A silicon sensor of thickness approximately  $280\mu\text{m}$  was placed in the setup, and measurements were taken of the sensor's response at full depletion. With trigger level running from 0.1 V to 1.25 V, at least  $10^4$  samples were taken for each trigger level. Approximately  $1.6 \times 10^4$  samples were also taken of the trigger response in this geometry. The dark count rate of the trigger was tested before data acquisition, and was found to be  $O(1 \text{ Hz})$  or less for trigger levels above 0.10 V, while the trigger rate with the source in place was  $O(30 \text{ Hz})$ . Therefore, noise has been treated as negligible.

To convert the output in voltage from the silicon sensor coupled to an amplifier, a series of scaling factors were applied:

$10^{-15} \text{ C}/0.012 \text{ V}$	Amplifier gain [4]
$6.241509 \times 10^{18} \text{ e}/\text{C}$	Electrons per Coulomb
$3.67 \text{ eV}/\text{eh}$	Average energy to produce e-h pair

Figure 10 shows the estimated MPV and FWHM of energy deposited in the sensor for varying trigger threshold voltage. A small inverse correlation of trigger threshold to both energy variables is noticeable. This may be indicative of the trigger successfully screening low-energy particles that are not minimum-ionizing.

The most probable value and full-width at half-maximum calculated from the measurements made in the actual setup were then compared to simulation for the same setup. As Figure 11 shows, the observed MPV energy deposited in the sensor by radiation from Sr-90 is approximately 0.9 times that of simulation. Figure 12 shows one example of the observed and simulated distributions for a trigger level of 1V, or 0.744 MeV deposited, equivalently. Precision on the FWHM is more limited due to sensitivity to binning in the calculation, but it is clear that the observed distributions have in general larger FWHM than simulation. Unfortunately,

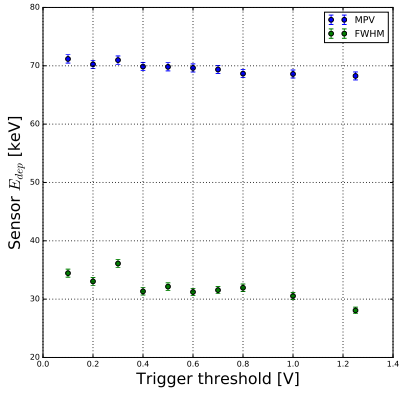


Figure 10: Output of 280  $\mu\text{m}$  sensor converted to keV.

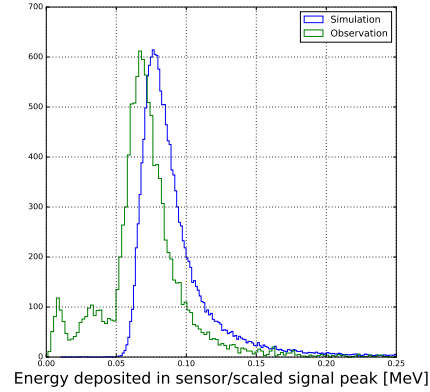


Figure 12: Simulated and observed distributions of sensor  $E_{dep}$ , 1V trigger.

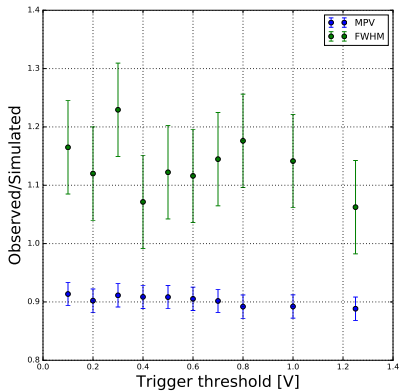


Figure 11: Ratio of estimated sensor  $E_{dep}$  to simulated.

Bichsel does not provide a full description of the expected energy loss in this energy range, so a direct comparison to theory cannot be made.

Due to limited availability of the Susi setup, only one sensor was measured. In principle this comparison between simulation and observation can and should be made for many sensor thicknesses, to examine the 'offset' of the MPV found in simulation across thicknesses. Figure 13 illustrates how the distribution in simulation changes with sensor thickness.

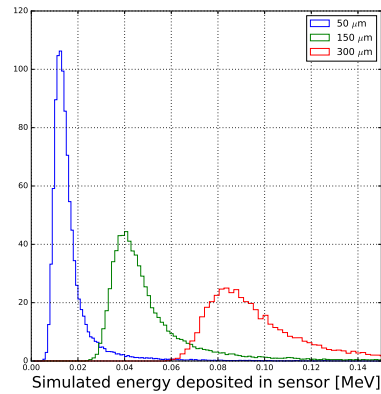


Figure 13: Distributions of sensor  $E_{dep}$  with varying thickness

## 6 Conclusions

Due to the stark difference between simulation and observation for tests with the Sr-90 source,

it seems clear that some aspect of the simulation has failed to capture the true experimental conditions. It is likely that this is a combination of effects from simulating a likely incorrect scintillator material and small details of the radioactive source's housing that have been incorrectly modeled.

However, the simulation predicts characteristics of the distribution of energy deposition in silicon sensors fairly well. For the MPV of this energy distribution, simulation is within approximately 10% of the values given by both theory and experiment. Simulation consistently underestimates the FWHM of the distribution by 10-15% when compared to theory and experiment.

To examine the issues laid out here in more detail, further steps should include taking data with other radioactive sources with varying characteristic radiation energy. This will allow a more precise determination of the relationship between trigger energy deposition and photo-multiplier output. The effects of the trigger condition should be examined for a wide range of sensor thicknesses. While there are still many questions to be answered and improvements to be made, GEANT4 simulation can clearly be a useful tool for studying the distribution of energy deposited in silicon detectors.

## References

- [1] Hans Bichsel. Straggling in thin silicon detectors. *Rev. Mod. Phys.*, 60:663–699, Jul 1988.
- [2] Esteban Curras Rivera. *Advanced silicon sensors for future collider experiments*. PhD thesis, Universidad de Cantabria, 4 2017. Section 3.3.
- [3] David-Leon Pohl. Source Simulation Software. <https://github.com/SiLab-Bonn/SourceSim>. Downloaded: 2017-07-04.
- [4] Cx Spectroscopic Amplifier. <https://cividec.at>. Accessed: 2017-08-18.